Development of a Demand Driven Hydro-climatic Model for Drought Planning

Mohammad Karamouz · Sanaz Imen · Sara Nazif

Abstract In recent years, droughts with increasing severity and frequency have been experienced around the world due to climate change effects. Water planning and management during droughts needs to deal with water demand variability, uncertainties in streamflow prediction, conflicts over water resources allocation, and the absence of necessary emergency schemes in drought situations. Reservoirs could play an important role in drought mitigation; therefore, development of an algorithm for operation of reservoirs in drought periods could help to mitigate the drought impacts by reducing the expected water shortages. For this purpose, the probable drought's characteristics and their variations in response to factors such as climate change should be incorporated. This study aims at developing a contingency planning scheme for operation of reservoirs in drought periods using hedging rules with the objective of decreasing the maximum water deficit. The case study for evaluation of the performance of the proposed algorithm is the Sattarkhan reservoir in the Aharchay watershed, located in the northwestern part of Iran. The trend evaluations of the hydro-climatic variables show that the climate change has already affected streamflow in the region and has increased water scarcity and drought severity. To incorporate the climate change study in reservoir planning; streamflow should be simulated under climate change impacts. For this purpose, the climatic variables including temperature and precipitation in the future under climate change impacts are simulated using downscaled GCM (General Circulation Model) outputs to derive scenarios for possible future drought events. Then a hydrological model is developed to simulate the river streamflow, based on the downscaled data. The results show that the proposed

M. Karamouz (✉)
Polytechnic Institute of NYU, Brooklyn, NY, USA
e-mail: karamouz@ut.ac.ir

S. Imen · S. Nazif
School of Civil Engineering, University of Tehran, Tehran, Iran

S. Imen
e-mail: sanazeimen@yahoo.com

S. Nazif
e-mail: snazif@ut.ac.ir

M. Karamouz
University of Tehran, Tehran, Iran

methodology leads to less water deficit and decreases the drought damages in the study area.

Keywords Climate change · Drought · Hydrological model · Downscaling · Hedging rules

1 Introduction

According to IPCC (International Panel on Climate Change) reports, climate change and global warming is occurring with different consequences all over the world (IPCC 2001). Due to the relationship between the hydrological cycle and climate system, every change on climate will affect hydrological variables such as precipitation and run-off, which directly affect water resources in a region and may result in some disasters such as drought or flash flood. Many studies have shown that the frequency and magnitude of extreme events are increasing around the world because of the climate changes (Mays 2003; Wigley and Jones 1985). Therefore monitoring these changes and planning water resources in accordance with these changes is a vital issue for development of a sustainable water supply scheme.

A combination of hydrometeorological variables such as precipitation and temperature can be used as an indicator for quantifying climate change impacts on water resources. Precipitation and temperature variations with respect to climate change effects are assessed using GCM (General Circulation Model) outputs. But the application of GCMs for the local impact studies is restricted because of their low spatial resolution (typically in the order of 50,000 Km^2) (Wigley et al. 1990; Carter et al. 1994). Therefore, downscaling techniques have emerged as a means to obtain local weather variables from regional atmospheric predictor variables. Harpham and Wilby (2005) simulated the precipitation for different zones of England using Statistical Down-Scaling Model, SDSM (Wilby et al. 2002), radial neural networks (neural networks with kernel based functions) and multi-layer perceptron neural networks. The results of their investigation show that all of these models are capable of simulating precipitation; however in different regions, their capabilities are different depending on the special characteristics of the region. Dibike and Coulibaly (2005) applied two statistical (a stochastic and a regression based) downscaling techniques called Long Ashton Research Station Weather Generator (LARS-WG) and Statistical Down-Scaling Model (SDSM) to generate the possible future values of local hydrometeorological variables such as precipitation and temperature in a watershed in the northern part of Canada. The results of this study show that GCMs are not very reliable in accuracy of simulated precipitation. Vidal and Wade (2008) investigated the uncertainty in catchment-scale precipitation scenarios due to the emissions scenario, the configuration of the GCM, and the downscaling method. The results show that the selection of a downscaling method and the multi-model building scheme has a significant impact on the simulated precipitation regime. Sajjad Khan et al. (2006) compared the results of three downscaling models namely SDSM, LARS-WG, and Artificial Neural Network (ANN), in terms of various uncertainty assessments exhibited in their downscaled results of precipitation and temperature. The uncertainty assessment results indicate that the SDSM is better capable of reproducing various statistical characteristics of the observed data. Massah Bavani (2006) used Kriging and the inverse weighting method for downscaling precipitation and temperature of the Zayandeh-rud river basin in Iran. His results indicate that both of these methods are capable of downscaling precipitation and temperature. Hingray et al. (2007) produced probability distributions for regional climate change in surface temperature and precipitation for 5 case studies. The results of regional climate changes especially at the end of study period (2070–

2099) are significantly different regarding to characteristics of case studies, seasons and meteorological variables.

To evaluate drought periods, it is important to convert rainfall to runoff as a basis for impact studies of water resources management practices and simulation of water availability in the future. Karamouz and Araghinejad (2008) integrated two models based on a fuzzy inference system (FIS) and an ANN model for long-term prediction of Zayandeh-rud river streamflow in Iran. They calibrated the fuzzy inference system to be used as a climatic model to predict seasonal rainfall. This was done through the effect of large scale climate signals on rainfall variation as well as the persistence of seasonal rainfall time series. ANNs were used to map the observed and forecasted hydroclimatologic data into the seasonal streamflow. In this study, after long lead stremflow prediction, the probable low flow periods (droughts) are characterized.

The appropriate on-time strategies should be used to decrease the social, economical, and environmental consequences of drought periods. The drought management has shifted to risk-based management as a critical approach to emphasize on mitigation of impacts associated with drought based on societal vulnerabilities. The main issue in water resources management during the drought period is the optimal operation of reservoirs and water storage facilities. One of the conventional methods used to mitigate drought impacts is limitation of water allocation from the reservoir potential even when there is enough water for full target supply but there are indications of probable drought in the near future. This method is called hedging rule. Hedging rule provides assurance for higher-valued water supply where the reservoirs have low refill potentials or uncertain inflows. The intent of hedging rule is to reduce the risk and the cost of large shortages, but accept the cost of more frequent small shortages. Hashimoto et al. (1982) showed that in the cases where the loss function (on releases) is linear, the SOP (Standard Operation Policy) could result in the best reservoir operation policy. Shih and ReVelle (1994) formulated a nonlinear mixed integer programming model that minimizes the maximum deficit while considering a constant demand. They converted the continuous hedging rule into multiple discrete hedging rules which are more appropriate for practical applications. Tu et al. (2003) developed an optimization model that incorporates both the rule curves and hedging rules for management and operation of a multiple, multi-purpose reservoir system. Draper and Lund (2004) demonstrated that the optimal hedging policy for reservoir operation depends on a balance between beneficial release and carry over storage values. Their results indicate that where hedging is desirable, a linear "two-point" hedging policy is a better choice in a wide range of circumstances.

In this paper, an integrated algorithm for applying contingency plan in reservoir operation in the Aharchay case study is developed considering the climate change impacts on streamflow to a reservoir. The main objective is to develop more economical monthly water supply scheme in the drought periods and make an assessment of climate change impacts on the reservoir ability to supply the demand.

In the following sections, the case study is introduced and it is followed by a description of the methodology of the study. Then, the results are presented and discussed. Finally, a summary and conclusion is given.

2 Case Study

Iran is located in a semi-arid region with considerable water shortage but less attention is given to reservoir operation in emergency situations caused by droughts. The static

operation rules which are commonly used, are not flexible and cannot be modified based on the observed situation; therefore, they may cause severe water shortages in droughts with high damages due to water shortages.

As a case study of this paper Sattarkhan reservoir, the only available surface water storage facility in the Aharchay river basin, in the northwestern part of Iran, has been selected. Aharchay river basin is located between 47°20′ and 47°30′ east longitude and 38° 20′ and 38°45′ north latitude. The location of the study area with an area of 950 (Km^2), is shown in Fig. 1. The mean annual rainfall and temperature at this basin are about 320 mm and 10°C, respectively. Sattarkhan reservoir has been in operation since 2000 and it is operated based on the standard operating policy (SOP) similar to most reservoirs in Iran (Fig. 7). The mean inflow of this reservoir is about 2.8 cm. The Reservoir is operated for multiple purposes, including water supply for irrigation, industrial, domestic uses, and instream (environmental) demands. The reservoir storage changes between 9 MCM (dead storage) and 132 MCM (maximum normal level). The average inflow to the reservoir is about 51 MCM/Year. The downstream demand of the Aharchay basin which is currently supplied by the Sattarkhan reservoir is about 50.52 MCM/year including water for irrigation (26.35 MCM/Year), industrial (5 MCM/Year), domestic (10.8 MCM/Year), and instream (environmental) demands (0.7 MCM/Year). It should be mentioned that the only considerable industrial activities in the study area is Songoon copper mine complex. The current irrigation area is about 3000 ha which will be increased to 8000 ha in the future. The projected water demand of the basin is shown in Table 1.

There are two meteorological stations, called "Kasanagh", a rain gage upstream of the reservoir and "Ahar", a synoptic station downstream of the reservoir, and a hydrometeorological station which is called "Orang", just upstream of the Sattarkhan reservoirs which in this study are called KH, AR, and OG stations, respectively. The characteristics of these stations are given in Table 2. Karamouz (2010) demonstrated that these stations can be considered as the representative of the meteorological and hydrological condition of the study area.

The GCM outputs that are necessary for evaluation of climate change effects are downloaded from http://www.cics.uvic.ca/scenarios. This site includes the HADCM3 GCM model outputs developed in the UK, for the location of the study region on the GCM model grid. The considered CO_2 emission scenarios are A2 and B2 which are both regional scenarios of climate change.
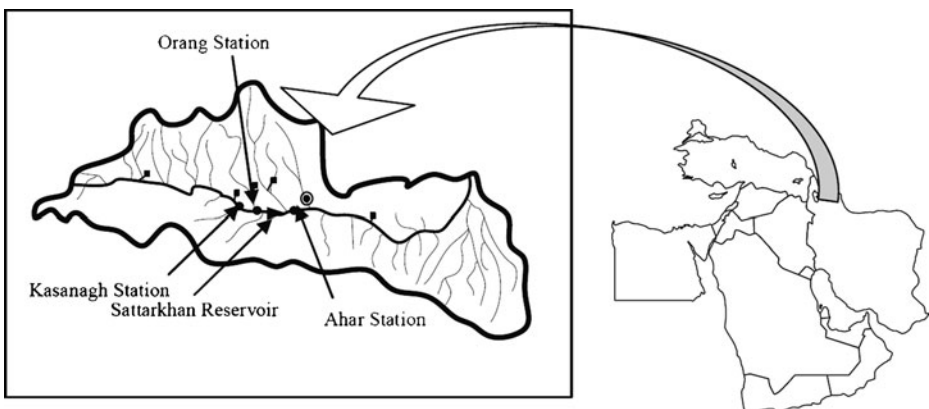
Fig. 1 The location of the study area on the map of Iran

Table 1 The projected water demands of the study area for different periods

| Year	Agricultural demand (MCM/year)	Industrial demand (MCM/year)	Domestic demand (Lit/day/person)
2016	70	5.31	223.4
2026	73.85	6.11	234.8
2036	77.63	7.16	246.8
2046	81.6	7.51	259.4

3 Methodology

In this paper, an algorithm has been developed to plan reservoir operation during the drought periods. The flowchart of the proposed methodology is shown in Fig. 2. Application of this methodology will increase the water supply system readiness to face the contingency periods of high water shortages. Since the water cycle characteristics change in time especially due to climate change effects, two examples of climate change scenarios are considered in order to project probable droughts' characteristics in future and examine the proposed method performance in future.

For simulation of future drought condition, it is necessary to simulate the streamflow and for this purpose simulation of rainfall and temperature is necessary. Based on Fig. 2, the future precipitation and temperature are simulated using the effective climatic predictors selected among HadGCM3 output data and through SDSM. The predicted rainfall is converted to the runoff by IHACRES (Identification of unit Hydrographs and Components from Rainfall, Evaporation and Streamflow) developed by the Integrated Catchment Assessment and Management (ICAM) centre of Australian National University to estimate inflow to the reservoir. This model performs well in simulation of streamflow and its variation scheme, but it is not capable of simulating the peak values. To overcome this shortcoming of IHACRES, a Multi Layer Perceptron (MLP) model of ANNs has been trained to modify the peak values.

Based on the estimated streamflow, water resources availability in the following years with respect to the growing water demand is evaluated. Then, drought indices of the SPI (Standardized Precipitation Index), SWSI (Surface Water Supply Index) and RDI (Reconnaissance Drought Index) are calculated to project the probable drought periods and their intensity in the future. Please see Morid et al. (2006), Karamouz et al. (2007, 2009), Karamouz and Araghinejad (2008), Clausen and Pearson (1995), Abbaspour and Sabetraftar (2005), Khalili et al. (2011), Tabrizi et al. (2010), Tsakiris and Vangelis (2005),

Table 2 The characteristics of the stations used in Aharchay basin

Station	Kasanagh (KH)	Ahar (AR)	Orang (OG)
Longitude	46–°51′	47–°04′	46–°52′
Latitude	38–°31′	38–°26′	38–°28′
Type of station	Rain gage	Synoptic	Hydrometric
Agency	Meteorological Organization of Iran	Meteorological Organization of Iran	Iran Ministry of power
Data period (years)	1971–2000	1986–2003	1983–2004
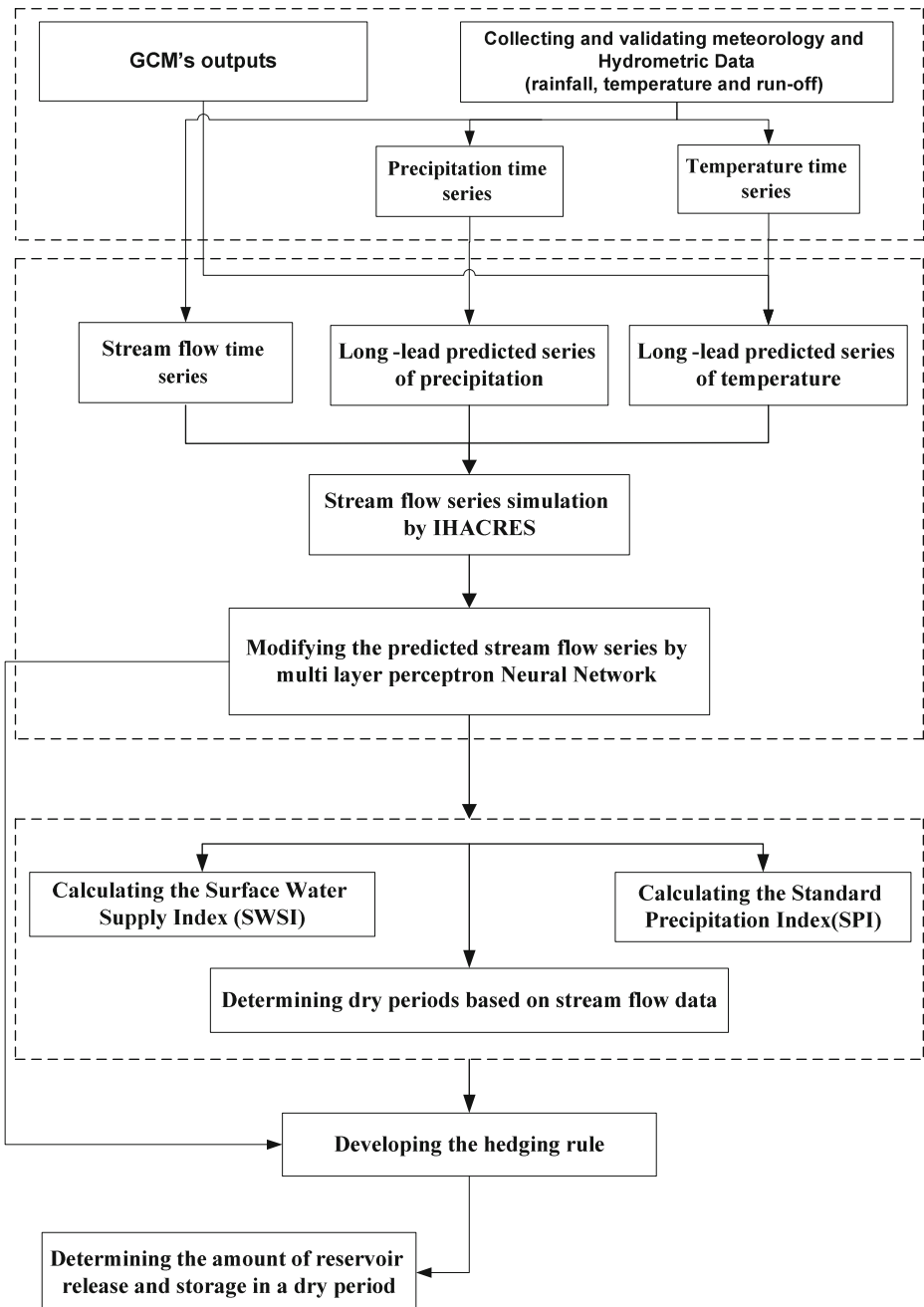
Fig. 2 The flowchart of reservoir operation using the climate change impacts on drought periods

Vangelis et al. (2010) and Tsakiris et al. (2006) for more information on SPI, SWSI and RDI and their applications for drought analysis in Iran and elsewhere. In the last step, the hedging rule is utilized to develop the reservoir operating policies during the projected

drought periods. In the hedging rule, a stationary reservoir operation scheme is provided to avoid the severe water shortage in case of long drought periods. In the following sections the methods and models used in this study are described.

3.1 Statistical Downscaling Method

In spite of the value of GCMs at the continental and hemispherical scales for assessing precipitation and temperature projections, they are inherently unable to demonstrate the characteristic and dynamics at the local sub-grid scale (Wigley et al. 1990; Carter et al. 1994). Therefore, GCM outputs should be converted into the local meteorological variables for reliable hydrological modeling. Methods used for this purpose are referred to as "downscaling techniques". A well recognized statistical downscaling tool that implements a regression based method is named SDSM (Wilby et al. 2002). The SDSM package is available at the Canadian climate impacts and scenarios project site (http://www.cics.uvis. ca/scenarios/). The most important advantages of the statistical downscaling method are the capability of working with limited data and the high speed of analysis. Full technical details of the SDSM are provided by Wilby et al. (1999). Within the classification of downscaling techniques, SDSM is best described as a hybrid of the stochastic weather generator and regression based methods. This is because large-scale circulation patterns and atmospheric moisture variables are used to linearly condition local-scale weather generator parameters. The downscaling algorithm of SDSM has been applied to a host of meteorological, hydrological and environmental assessments, as well as a range of geographical locations such as Europe, North America and Southeast Asia (Hassan et al. 1998; Wilby et al 2000; Hay et al. 2000). The stochastic component enables generation of multiple simulations with slightly different time series attributes, but the same overall statistical properties. This downscaling method has been widely used within the climate impact community (Dibike and Coulibaly 2005; Wilby and Harris 2006; Prudhomme 2006). Using the daily GCM outputs, daily rainfall series are generated for future years using SDSM in which a multiple linear regression is developed between selected large-scale predictors and a local scale predictands such as temperature or precipitation in each month. The parameters of the regression equations are estimated using the efficient dual simplex algorithm. Large-scale relevant predictors are selected using correlation analysis, partial correlation analysis and scatter plots considering physical sensitivity between selected predictors and predictands in the region.

For precipitation downscaling, the predictors describing atmospheric circulation such as thickness (different atmospheric layers), different indices of wind velocity such as vorticity, zonal velocity and moisture content such as specific and relative humidity, in different altitudes, are preferred (Wilby et al. 2002). The utilization of SDSM includes five distinct tasks: (1) preliminary screening of potential downscaling predictors; (2) assembly and calibration of SDSM; (3) synthesis of ensembles of current weather data using observed predictor variables; (4) generation of ensembles of future weather data using GCM-derived predictor variables; (5) diagnostic testing/analysis of the observed data and climate change scenarios. In this study SDSM version 3.1 has been used.

3.2 IHACRES Model

There are different hydrological models used for rainfall-runoff modeling with special characteristics and limitations. Jakeman and Hornberger (1993) showed that the IHACRES model could be applied to a river basin with limited data of acceptable accuracy. This model requires river basin size (m^2), time series of daily rainfall, daily

streamflow data for model calibration and a surrogate variable representing evaporation where daily air temperature data is usually used. The model simulates the daily streamflow based on the input data.

The procedure followed in this model to convert rainfall to runoff. First, the recorded rainfall, r_k, is converted to effective rainfall u_k using a non-linear loss module.

$$u_k = S_k * r_k \tag{1}$$

where S_k (river basin wetness index) is computed at each time step k on the basis of recent rainfall and temperature as follows:

$$S_k = C \times r_k + \left(1 + \frac{1}{\tau_w(t_k)}\right) S_{k-1} \tag{2}$$

$$\tau_w(t_k) = \tau_w e^{0.062 f(R - t_k)} \tag{3}$$

where R is the reference temperature and C is determined based on the mass balance between effective rainfall and runoff in the calibration period. $\tau_w(t_k)$ is always more than one and $S_0=0$. The underlying conceptualization of this module is that a river basin's wetness varies with recent rainfall and evapotranspiration. Two major parameters in this model are τ_w and f. Parameter τ_w (the river basin drying time constant) is a value of $\tau_w(t_k)$ at a reference temperature, in which $\tau_w(t_k)$ controls the rate in which the river basin wetness index (S_k) decays in the absence of rainfall. Parameter f (the temperature modulation factor) controls the sensitivity of $\tau_w(t_k)$ to changes in temperature, t_k. In the second step, a linear unit hydrograph (UH) module converts effective rainfall to streamflow, X_k.

The linear module allows the application of the well-known unit hydrograph theory which conceptualizes the river basin as a configuration of linear storages acting in series and/or parallel. The configuration of linear storage in the UH module which is allowed in IHACRES includes single storage and two storage units, in series or parallel. The optimal pair of (τ_w, f) is identified by trial and error for a given configuration of simple UH's and a given value of the pure time delay between rainfall and runoff occurrence. Then the model automatically estimates the relevant parameters for a subsequent simulation.

3.3 Hedging Rule

Hedging is known as a means of withholding water before and during the drought periods (Bower et al. 1962). Therefore a lower deficit is accepted in the current supply in order to avoid more severe water shortages in the following periods. The hedging rule is the reservoir operation rule, which reduces deliveries of some portion of water supply to retain storage for use in the dry periods and provide assurances for higher priority water usage when the reservoir has low refill potential or uncertain inflows. As it is shown in Fig. 3, during normal periods of operation, when inflows are high and the reservoir is almost full, the operating rule efficiently allocates water to meet the demands imposed by competing users. During a drought, or when a drought is anticipated, as the reservoir inflow decreases and reservoir storage drops, the planned demands cannot be fully met. By considering the hedging rules along with the rule curves, guidelines are provided for reservoir release. To minimize the impact of drought, the hedging rules effectively reduce the ongoing water supply rate to offset the target storage to its target requirement.

Based on Lund and Guzman (1996), there are three types of hedging rules as follows (Fig. 3):

- One-point hedging: In this model, the water release starts from nothing and increases linearly (at a slope <1) until intersecting with the actual water demand (Shih and Revelle 1994)
- Two-point hedging, where a linear hedging rule begins from a first point (parameter) occurring somewhere above the origin on the shortage portion of the SOP rule to a second point occurring where the hedging slope (<1) intersects with the actual water demand (Bayazit and Unal 1990; Srinivasan and Philipose 1996)
- Three-point hedging, where an intermediate point is specified in the two-point hedging rule, introducing two linear portions to the hedging portion of the overall release rule.

Draper and Lund (2004) tested the three types of hedging rules and concluded that the two point hedging rule is better in comparison with other hedging rules. Therefore, in this study, the two point hedging rule is employed. To develop hedging rules, the model proposed by Tu et al. (2003) is extended considering two distinct water demand categories. The objective function of this model is maximizing the water allocation to water demand categories as well as the reservoir storage.

$$MAX \quad \sum_{t=1}^{T} \left(RP_t.W_p + RA_t.W_a + St_t.W_s \right) \tag{4}$$

where T is the decision time period duration (months), RP_t is the allocated water to industrial, municipal, and instream demands, namely overall public demand, in month t, RA_t is the
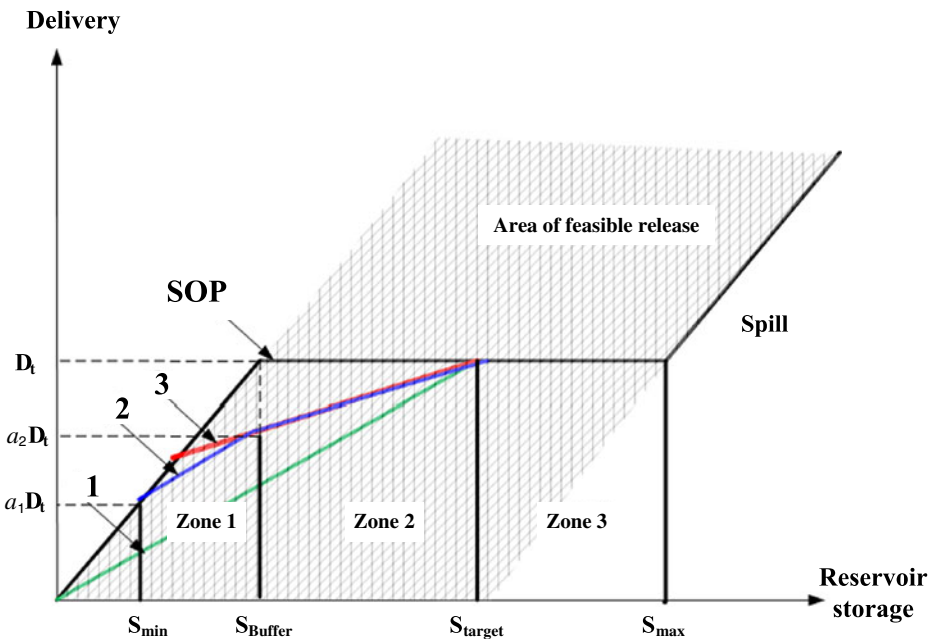

Fig. 3 Different types of Hedging rules in comparison with the Standard Operation Policy (SOP) and the conservation scheme of operation rules

allocated water to agricultural demand in month t, St_t is the reservoir storage at the beginning of month t and W_p, W_a and W_s are weighting factors for public demand, agricultural demand and reservoir water storage, respectively. In this study, the weighting factors for public demand, agricultural demand and reservoir water storage are considered as 0.55, 0.25, and 0.2 respectively based on the priorities and stakeholders' dependencies for different sectors.

The following assumptions are made in developing the optimization model: (1) All of water demand is supplied from the surface water (2) No loss occurs in domestic water supply. In order to apply hedging rules in reservoir operation, a set of constraints are defined as follows:

$$St_t + I_t - R_t - E_t = St_{t+1} \tag{5}$$

$$St_{min} \leq St_t \leq St_{max} \tag{6}$$

$$St_t = \lambda_{1t}St_{1,t} + \lambda_{2t}St_{2,t} + \lambda_{3t}St_{3,t} \tag{7}$$

$$\lambda_{1,t}.St_{min} \leq St_{1,t} < \lambda_{1,t}.St_{Buffer} \tag{8}$$

$$\lambda_{2,t}.St_{Buffer} \leq St_{2,t} < \lambda_{2,t}.St_{target} \tag{9}$$

$$\lambda_{3,t}.St_{target} \leq St_{3,t} \leq \lambda_{3,t}.St_{max} \tag{10}$$

$$R_t \leq \left(\lambda_{1,t}.\alpha_1 + \lambda_{2,t}.\alpha_2 + \lambda_{3,t}\right).D_t \tag{11}$$

$$\lambda_{1,t} + \lambda_{2,t} + \lambda_{3,t} = 1 \tag{12}$$

$$\lambda_{1,t} = \begin{cases} 1 & \text{if } st_t \text{ is in zone 1} \\ 0 & \text{otherwise} \end{cases} \tag{13}$$

$$\lambda_{2,t} = \begin{cases} 1 & \text{if } st_t \text{ is in zone 2} \\ 0 & \text{otherwise} \end{cases} \tag{14}$$

$$\lambda_{3,t} = \begin{cases} 1 & \text{if } st_t \text{ is in zone 3} \\ 0 & \text{otherwise} \end{cases} \tag{15}$$

where I_t is inflow; R_t is reservoir release; E_t is evaporation loss from the reservoir; all of them in month t. St_{min} is the minimum storage of the reservoir; St_{max} is maximum storage of the reservoir; S_{target} is target storage; S_{Buffer} is buffer storage; D_t is water demand at month t; $\lambda_{1,t}$, $\lambda_{2,t}$ $\lambda_{3,t}$ are binary variables which determine the reservoir storage class (which are

described in the following paragraph) according to Fig. 3; α_1, α_2 are rationing factors used in order to limit the water supply in dry periods as shown in Fig. 3. In this study, reservoir storage is divided into four pools. These include, from top to bottom, the flood-control zone (S_{max} to S_{target}), conservation zone (S_{target} to S_{buffer}), buffer zone (S_{buffer} to S_{min}) and inactive zone (less than Smin(.The storage between conservation and buffer pools, together, constitute the reservoir's active storage. The buffer zone is determined based on the reservoir volume at the level of the lowest (first) reservoir outlet for water supply and the conservative zone corresponds to the volume below the top of the second reservoir outlet. Based on the design characteristics of Sattarkhan dam, minimum storage, maximum storage, target storage, and buffer storage are considered as 9, 132, 57.5, and 24 respectively.

The continuity equation for the reservoir is written as Eq. 5. During each time period t, the relationship between the rule curve and the hedging rule is shown as the step function (Fig. 3). According to Fig. 3, the storage volume is divided into three classes where the first class varies between the minimum storage and buffer levels, the second class is between buffer and target storage levels, and the volume between target and maximum storage levels is considered as the third class.

In each time period the amount of the reservoir storage, St_t, will be placed in one of these three classes (Eqs. 8, 9 and 10). To define the storage class in the modeling process, three binary variables of $\lambda_{1,t}$, $\lambda_{2,t}$, $\lambda_{3,t}$, are determined using Eqs. 13 to 15. Equation 12 ensures that in each time step only one of the $\lambda_{1,t}$, $\lambda_{2,t}$, $\lambda_{3,t}$ could be active regarding to the reservoir storage class. With respect to the activated binary variable, the appropriate hedging rule for water release is developed. In the developed hedging rule, two rationing variables α_1, α_2 are used to determine the percentage of the supplied demand depending on the reservoir storage class (Eq. 11). The rationing variables are determined at the planning stage and could be modified to meet operational purposes in different situations.

As it is shown in Fig. 3, when the reservoir storage falls below the target storage, while employing the hedging rule, the reservoir release is reduced regarding the severity of drought in order to provide a sustainable water supply scheme during the drought period. But in application of the SOP strategy, if the water supply is less than the target demand D_t, all available water is released; no storage remains.

4 Results

4.1 Rainfall Projection Under Climate Change Impacts

The results of statistical downscaling are highly dependent on the assumption that the data is outlier-free, nearly normal, and the data is not serially correlated. If the applied data does not satisfy these assumptions, the results may be misleading. Therefore, the adequacy of data is checked at the first step. Based on the statistical evaluation of data, there was no outlier in the collected data. The normality test of rainfall and temperature data showed the need for using transformation for normalizing the data. Among different transformation methods, the fourth root transformation has been selected to normalize both the rainfall and temperature data. The autocorrelation analysis of rainfall data using ACF (Autocorrelation Function) diagrams at different lag times did not show any significant correlation in the 95% confidence level. The same analysis for temperature data showed that the first serial correlation is significant. These revealed characteristics are considered in further evaluation of the downscaling results.

To select the best set of rainfall predictors in the region, the relation between different combinations of climatic predictors and regional rainfall has been examined through evaluation of physical relationship and statistical tests. The results showed that different combination of predictors should be used for rainfall simulation in different months of a year. This is due to different climatic systems that affect rainfall variations during a year. In fact, the first group includes two predictors: Relative 500 hPa (hectopascal) Geopotential Height and Humidity at 500 hPa. These predictors are used for rainfall projection of all months except April, May and June (spring season). The predictors of the second group that are used to project spring rainfall include surface divergence, mean sea level pressure and 500 hPa vorticity.

The downscaling model has been calibrated during 1971–1980 and the results have been validated for 10 years during 1981–1990. Global reanalysis of NCEP (National Centers for Environmental Prediction) are used to find relationships between large-scale predictors and local predictands in model calibration. The NCEP reanalysis data are developed by NCEP and National Center for Atmospheric Research (NCAR) through a project (denoted "reanalysis") and produce a retroactive record of more than 50 years of global analyses of atmospheric fields in support of the needs of the research and climate monitoring communities.

4.1.1 BSS Quantification

In this study, 20 ensembles of future rainfall and temperature series are developed arbitrarily. Due to large number of ensembles, each of which have long time periods, the most appropriate ensemble among generated data is selected for further analysis. For this purpose the Briers Skill Score (BSS) is employed. BSS compares different set of model predictions, Y, against a baseline prediction, B, and a set of model observations, X, and is estimated as follows (Spearman et al. 2004),

$$BSS = 1 - \frac{MSE(X, Y)}{MSE(B, X)} \tag{16}$$

where $MSE(X,Y)$ is the mean square error given by $MSE(X, Y) = \frac{1}{n} \sum (Y_i - X_i)^2$. The BSS gives a value of 0 if the prediction set of Y is as well as the baseline prediction, B. The BSS gets a maximum value of 1 if the prediction set of Y is 100% accurate (i.e. $Y=X$) and a negative score if the prediction set of Y is worse than the baseline. In this study, the first ensemble has been considered as baseline prediction and other ensembles are compared with it. The results are tabulated in Table 3. Based on this table, the 9th, 14th and 20th ensembles of NCEP, Had A2 and Had B2 rainfall downscaling data are selected respectively, for further analysis. They have the maximum value of BSS in each case.

In Fig. 4, the monthly mean of downscaled (using NCEP data) and observed rainfall are compared. The maximum difference between the observed and simulated monthly rainfall is about 15% in February. The downscaling results are underestimated in August-November and overestimated in the other months, but the differences are not significant.

To ensure the appropriate performance of the downscaling model, regarding to the characteristics of the observed data, nonparametric methods are employed to test the equality of mean and variance of the downscaled and observed data. The applications of these tests are discussed in the following sections.

Table 3 The results of BSS calculation to select the most appropriate ensembles of downscaled data of rainfall and temperature

Ensemble prediction		2	3	4	5	6	7	8	9	10	11	12	13	14	15	16	17	18	19	20
Rainfall	NCEP	-0.01	0.04	0.03	0.00	-0.03	0.01	-0.03	0.06	-0.01	0.00	0.03	0.03	0.03	-0.03	-0.21	-0.08	0.04	0.00	-0.12
	Had A2	-0.05	-0.11	-0.02	0.11	0.09	-0.12	-0.07	-0.10	0.05	-0.12	-0.08	-0.14	0.12	0.00	-0.11	-0.01	-0.08	-0.03	0.00
	Had B2	0.14	0.10	0.07	0.00	0.07	-0.05	0.01	0.05	0.02	0.00	0.05	0.05	-0.01	0.06	-0.09	-0.06	-0.01	0.10	0.15
Temperature	NCEP	-0.05	-0.09	0.06	0.02	0.05	-0.01	-0.06	-0.02	-0.04	0.12	0.06	-0.05	-0.01	0.08	-0.12	0.08	0.06	-0.04	0.10
	Had A2	0.03	0.11	-0.05	-0.01	-0.05	0.01	-0.08	0.09	-0.04	-0.15	0.06	-0.10	-0.08	0.06	0.15	-0.03	0.05	-0.06	-0.02
	Had B2	-0.12	-0.10	0.09	0.05	0.17	-0.12	0.06	-0.11	-0.02	0.09	0.15	-0.05	0.06	-0.02	0.10	0.08	-0.05	0.12	-0.11
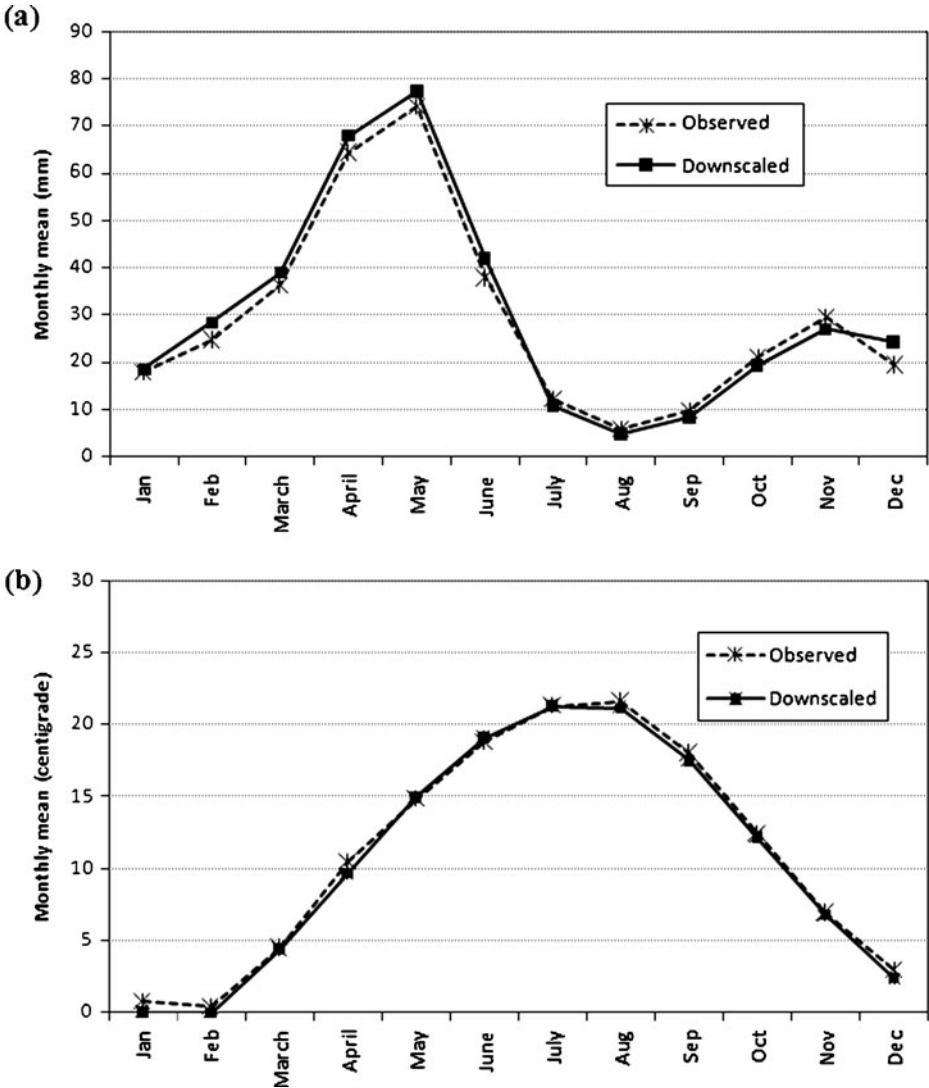
Fig. 4 Comparison between the monthly mean of downscaled and observed **a** rainfall (1971–2000) **b** temperature (1986–2000)

4.1.2 Wilcoxon Rank Sum Test

For constructing a hypothesis test p-value for equality of means of observed and downscaled data (difference of two population means), the Wilcoxon rank sum method is used (Sajjad Khan et al. 2006; Conover 1980). A detailed description of the theory of Wilcoxon rank sum test can be found in Conover (1980). In terms of hypothesis testing, p-value is the level of significance for which observed test statistic lays on the boundary between acceptance and rejection of the null hypothesis (equality of means). At any significance level greater than the p-value, the null hypothesis is rejected, and at any

significance level less than the p-value the null hypothesis is accepted. MATLAB 7.0 software is used for performing this test. The results of this test application are given in Table 4. As can be seen, the results are all meaningful in 5% significance level except in May and April.

4.1.3 Modified Levene's Test

Modified Levene's test suggested by Brown and Forsythe (1974) is used in this study to test the equality of variance of downscaled and observed data. Modified Levene's test is used when the data come from continuous, but not necessarily normal, distributions. In this method the distances of the observations from their sample median are calculated (Sajjad Khan et al. 2006). MINITAB 13.0 is used for performing Modified Levene test. The results of this test are the same as the Wilcoxon text (Table 4). The null hypothesis of accepting the variance is rejected at 5% significance level in months of May and April when the downscaled data are accepted within 1% significance level.

In Table 5, the monthly maximum, minimum, mean, and variance of observed and downscaled rainfall are compared during 1971–2000. Based on these results, the developed model could be used to simulate the monthly rainfall pattern of the study area.

Massah Bavani (2006) demonstrated that HadCM3 GCM model has the best performance in application to Iran climate change assessment studies. Then the outputs of HadCM3 GCM model for Had A2 and Had B2 climate change scenarios are imported to SDSM software to exemplify the probable changes of region climate under climate change impacts.

In Table 6, the scenarios Had A2 and Had B2 are compared with the observed rainfall data during 1971–2000. Since there is no significant difference between results of two climate change scenarios, the results of scenario Had B2 are used for further analyses. In Fig. 5, the monthly mean of observed and Had B2 scenario results are compared during the period of 1971–2000. The investigation of climate change scenarios on the rainfall shows that the rate of rainfall fluctuates with a decreasing trend.

4.2 Future Temperature Projection

Since temperature data is needed in the rainfall-runoff modeling by IHACRES model, it has been downscaled in this study using the same procedure as rainfall downscaling. Two predictors of 500 hPa geopotential height and mean sea level pressure have been identified for temperature simulation. The model has been calibrated for years 1986–1995 (because of the availability of the observed data in this period) where the correlation coefficient between effective predictors and temperature in the calibration period is 76% which is significant in climate studies. The model is validated for period of 1996–2000. The better ensembles of downscaled temperature data are selected based on calculated BSS for different scenarios (Table 3). The monthly mean of downscaled and observed temperature are compared in Fig. 4.

In order to test the equality of mean and variance of the downscaled and observed temperature data, the Levene and Wilcoxon rank sum tests are employed (Table 4). The results of some months do not satisfy the criteria of mean and variance equality of observed and downscaled data but since temperature data is only used as an indicator for considering snow melt in rainfall-runoff model, the downscaled data could be applied with the current level of accuracy.

Table 4 The results of performing Levene and Wilcoxon rank sum tests to evaluate the performance of downscaling model in simulating temperature and rainfall data in the study area

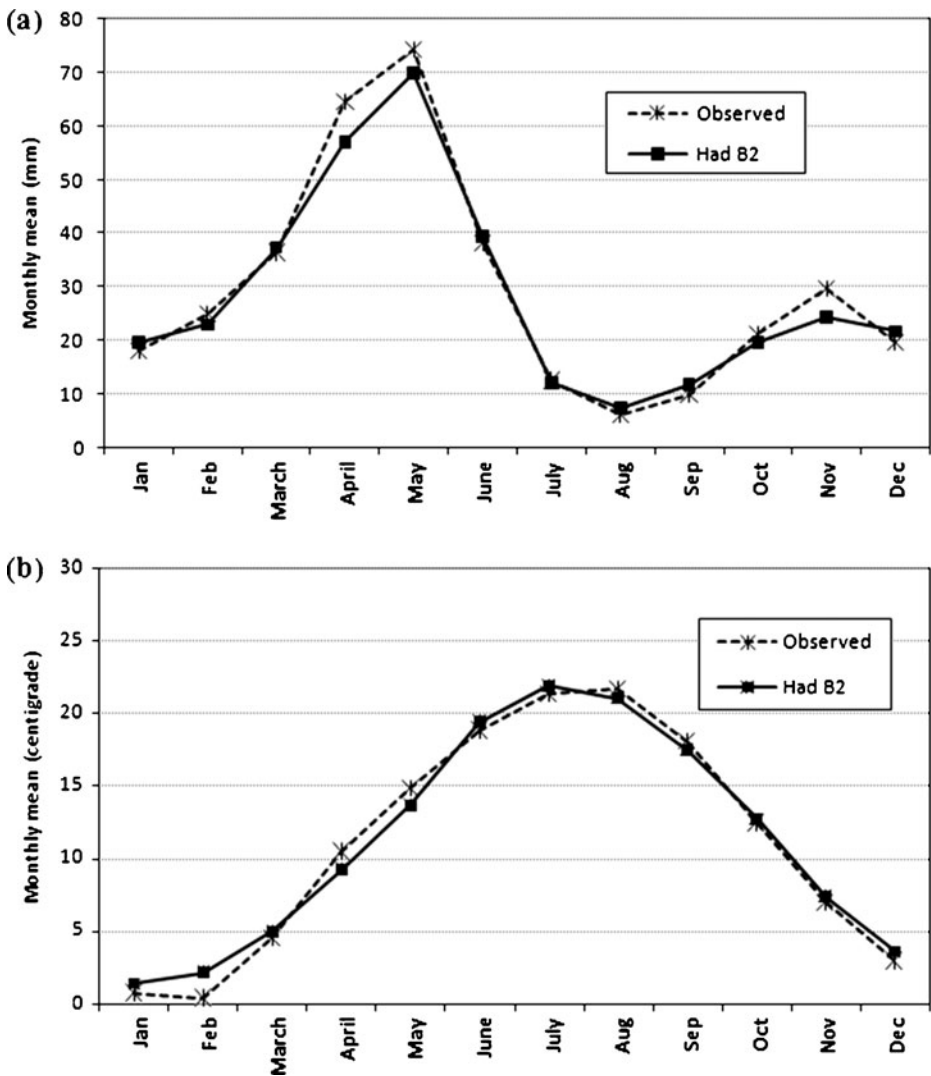| Scenario	Month	Rainfall			Temperature		
		Levene test		Wilcoxon rank sum test	Levene test		Wilcoxon rank sum test
		Statistics	p-value	p-value	Statistics	p-value	p-value
NCEP	Jan.	0.194	0.659	0.620	0.173	0.678	0.058
	Feb.	0.498	0.481	0.410	0.848	0.358	0.127
	Mar.	0.494	0.482	0.490	0.713	0.135	0.004
	Apr.	0.942	0.332	0.041	0.387	0.534	0.032
	May.	9.871	0.002	0.006	1.127	0.289	0
	Jun.	0.826	0.363	0.155	0.36	0.549	0
	Jul.	0.089	0.766	0.379	3.175	0.076	0.001
	Ague.	0.466	0.495	0.684	1.473	0.226	0.096
	Sep.	0.577	0.447	0.582	0.648	0.421	0.029
	Oct.	1.358	0.244	0.284	1.573	0.21	0.036
	Nov.	0.02	0.888	0.594	7.143	0.008	0
	Dec.	0.056	0.813	0.835	1.128	0.384	0.220
Had A2	Jan.	2.467	0.116	0.041	0.084	0.772	0
	Feb.	0.099	0.753	0.987	0.281	0.596	0
	Mar.	0.041	0.839	0.951	4.164	0.046	0.168
	Apr.	12.03	0.001	0.010	20.267	0	0
	May.	22.529	0	0	66.416	0	0.010
	Jun.	1.579	0.209	0.245	19.331	0	0
	Jul.	0.719	0.397	0.807	35.246	0	0
	Ague.	0.611	0.435	0.148	66.821	0	0
	Sep.	0.026	0.871	0.833	10.028	0.002	0.170
	Oct.	0.058	0.81	0.959	46.883	0	0.179
	Nov.	0.998	0.318	0.692	8.923	0.003	0
	Dec.	1.843	0.175	0.271	1.118	0.291	0
Had B2	Jan.	1.735	0.188	0.017	2.856	0.091	0
	Feb.	0.042	0.837	0.896	3.345	0.064	0
	Mar.	2.87	0.091	0.033	7.807	0.005	0
	Apr.	7.725	0.006	0.010	43.335	0	0.006
	May.	1.75	0.188	0.711	42.655	0	0.016
	Jun.	4.179	0.041	0.021	16.176	0	0
	Jul.	1.656	0.198	0.627	29.875	0	0
	Ague.	0.481	0.488	0.544	43.629	0	0.728
	Sep.	0.024	0.876	0.849	10.296	0.001	0.703
	Oct.	0.412	0.521	0.410	65.204	0	0.001
	Nov.	3.552	0.06	0.121	13.91	0	0
	Dec.	3.154	0.076	0.092	0.817	0.366	0

Since there is no significant difference between results of two considered climate change scenarios and for compatibility with rainfall data, the result of scenario Had B2 has been

Table 5 Comparison between observed and simulated rainfall data (in mm, 1971–2000)

Month	Maximum		Minimum		Mean		Variance	
	Observed	Downscaled	Observed	Downscaled	Observed	Downscaled	Observed	Downscaled
January	23.00	45.35	0.50	0.37	4.98	5.39	5.87	7.40
February	26.00	26.98	1.00	0.50	4.85	4.58	6.70	5.86
March	21.01	26.23	1.00	0.43	5.42	5.48	8.37	9.28
April	29.02	34.07	1.00	0.63	6.50	6.90	12.98	15.07
May	43.02	44.07	1.00	0.27	7.72	8.57	25.14	38.90
June	34.01	36.18	1.00	1.48	7.83	6.96	11.99	12.96
July	10.78	14.87	1.00	0.29	4.97	5.70	0.89	0.94
August	59.99	54.11	1.00	0.29	6.38	5.49	5.56	4.70
September	26.00	23.73	1.50	0.74	6.18	5.19	3.53	4.83
October	26.00	23.85	1.50	1.23	6.38	6.09	8.00	6.09
November	34.01	29.02	1.00	0.78	5.77	5.64	7.80	10.20
December	35.97	39.94	1.00	0.86	5.48	5.30	9.05	9.84

Table 6 Comparison of observed rainfall data with Had A2 and Had B2 (in mm, 1971–2000)

Month	Maximum			Minimum			Mean			Variance		
	Observed	Had A2	HadB2	Observed	Had A2	HadB2	Observed	Had A2	HadB2	Observed	Had A2	HadB2
January	23.00	27.55	30.08	0.50	0.36	0.49	4.98	4.88	4.88	5.87	7.29	4.77
February	26.00	21.21	20.35	1.00	0.88	0.84	4.85	5.48	5.10	6.71	9.01	8.56
March	21.01	33.45	18.93	1.00	1.12	0.83	5.42	5.55	5.54	8.37	5.49	8.38
April	29.02	30.92	30.16	1.00	0.95	0.94	6.50	6.84	6.46	12.84	17.55	12.32
May	43.02	55.02	45.02	1.00	0.46	0.84	7.72	10.13	8.87	25.14	39.81	37.22
June	34.01	65.51	34.81	1.00	0.70	0.77	7.83	7.30	7.97	11.99	16.62	15.07
July	10.78	12.13	11.65	1.00	0.56	0.78	4.97	4.66	4.39	0.89	2.44	1.42
August	59.99	46.12	55.54	1.00	0.32	1.00	6.38	3.03	5.82	5.56	2.089	4.22
September	26.00	29.42	29.27	1.50	1.10	1.48	6.18	5.28	5.92	3.53	2.40	3.64
October	26.00	29.83	25.70	1.50	0.92	1.30	6.38	6.74	5.98	8.06	6.79	7.85
November	34.01	37.10	32.68	1.00	0.82	0.83	5.77	6.01	5.44	7.82	9.53	10.48
December	35.97	25.49	25.18	1.00	0.46	0.84	5.48	4.75	5.72	9.05	5.37	4.43

Fig. 5 Comparison between the monthly mean of Had B2 scenario and observed **a** rainfall (1971–2000) **b** temperature during (1986–2000)

used for further analyses. The comparison between monthly mean of Had B2 scenario and observed temperature is shown in Fig. 5. The investigation of climate change effects on the temperature during 2004–2042 shows that there is an increasing trend in the temperature as there is an almost 0.8 centigrade degree increase each 20 years after 2004 (the final year of available data for this study).

4.3 Runoff Prediction Using Rainfall-Runoff Model

Parameters f, τ_w, δ (time delay) and the hydrograph condition are determined by trial and error to minimize the runoff simulation error in the calibration period. Two indices of

coefficient of determination, D, and percentage average relative parameter error, $ARPE$, are used to determine the simulation error when calibrating IHACRES. High D and low $ARPE$ are desirable. These parameters are formulated as follows.

$$D = 1 - \frac{[\sigma_\xi]^2}{[\sigma_y]^2} \tag{17}$$

$$ARPE = \left[\left[\frac{\sigma_{a1}}{a_1}\right]^2 + \left[\frac{\sigma_{a2}}{a_2}\right]^2 + \left[\frac{\sigma_{bo}}{b_0}\right]^2 + \left[\frac{\sigma_{b1}}{b_1}\right]^2 \right]/4 \tag{18}$$

where σ denotes standard deviation and, ξ and y subscripts correspond to model residuals and observed streamflow, respectively. The parameters of Eq. 18 are calculated using Eqs. 19 to 22, in which b and a are the unit hydrograph (UH) parameters and, s and q stand for slow and quick unit hydrographs, respectively.

$$b_0 = b_0^{(q)} + b_0^{(s)} \tag{19}$$

$$b_1 = b_0^{(q)} a_1^{(s)} + b_0^{(s)} a_1^{(q)} \tag{20}$$

$$a_1 = a_1^{(q)} + a_1^{(s)} \tag{21}$$

$$a_2 = a_1^{(q)} . a_1^{(s)} \tag{22}$$

Consider the simple discrete-time hydrograph in which unit effective rainfall over one time step produces streamflow ($b<1$) over the same time step. In each subsequent time steps, streamflow is a fixed proportion ($a<1$) of what it was in the previous time step and thus the flow decays exponentially (at a rate determined by a). In this study, the rates of exponential decay for the two simple UHs, one is 'quick' (q) and another is 'slow' (s), that are combined to give a UH for total streamflow. In Eqs. 19 to 22, $b_0^q > 0$, $-1 < a_1^q < 1$ and $b_0^s > 0, -1 < a_1^s < 1$ are the quick and slow streamflow components of UH, respectively.

In the non-linear loss module, the ranges are selected for the parameters f and τ_w. For each pair of these parameters, D and $ARPE$ are calculated to select the best pair. In this study, τ_w has been changed in the range of 1–100 by using a model step of 1 and the range of 1–10 has been considered for variations of f by using model step of 0.1. Finally, values of 3.2, 5 and 0 are estimated for parameters f, τ_w and δ, respectively based on D and $ARPE$ parameters. In addition a single hydrograph scheme has been determined as the best system that presents the rainfall-runoff process in the basin.

The accurate determination of the calibration period is important in achieving accurate simulation of basin runoff using the IHACRES model; therefore, different calibration periods are checked and finally the period of 1988–1997 is selected in developing the final

runoff simulation model. Because of the missing data in the OG station between years 1999 to 2000, the model has been validated for the period of 2002–2004.

The daily simulated runoff data using IHACRES are converted to monthly timescales in order to be used in reservoir optimization model. The results of runoff simulation in the calibration and validation periods in the monthly time scale are shown in Fig. 6. According to this figure, although this model can simulate the value and trend of runoff, it is not capable of simulating the peak values. This could be due to simplifications made in this model which could not consider some phenomena affecting runoff variations such as snow budget or flash floods. To improve the results of the IHACRES model in simulating the extreme values, a Multi Layer Perceptron (MLP) model of ANNs has been trained.

The inputs of MLP model are the observed rainfall and runoff in the present month and the simulated runoff by IHACRES for the next month, and the output is the modified runoff for the next month. The MLP with one hidden layer has been trained for the period of 1988–1997. The years between 1997 and 2000 are not considered in the model calibration due to lack of data during these years that may result in high errors in the model performance. The optimal number of neurons in the hidden layer and training epochs has been determined by trial and error. The range of 2–15 has been checked for the number of neurons in the hidden layer and training epochs between, 500 and 4,000 by 500 steps has been considered. Finally, 12 neurons in the hidden layer and training epoch of 500 have been chosen.

The results of the MLP model have been compared with the observed values as shown in Fig. 6 for calibration and validation periods. The comparison between parts (a) and (b) of the Fig. 6 demonstrates that the percentage of error in MLP model is 13% less compared to the IHACRES model.
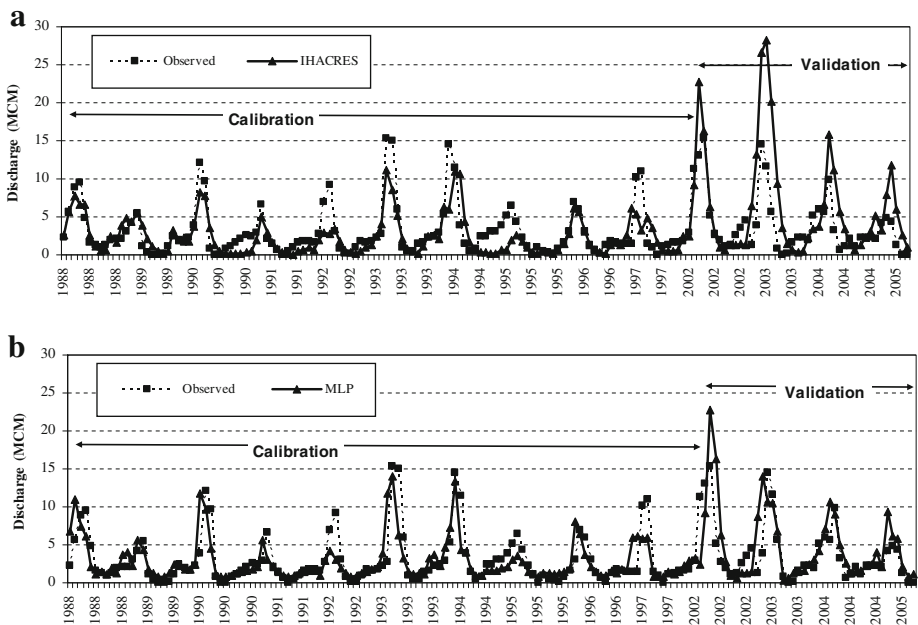
Fig. 6 Comparison between the monthly observed run-off and (**a**) IHACRES simulated, (**b**) MLP simulated in calibration and validation period

The performances of developed models are evaluated based on E (Nash–Sutcliffe model efficiency coefficient), MAE (Mean Absolute Error) and RMSE (Root Mean Square Error) indices as demonstrated in Table 7. These indices are quantified as follows:

$$MAE = \frac{\sum\limits_{t=1}^{n} \left| X_p^t - X_o^t \right|}{n} \tag{23}$$

$$RMSE = \sqrt{\frac{\sum\limits_{t=1}^{n} \left(X_p^t - X_o^t \right)^2}{n}} \tag{24}$$

$$E = 1 - \frac{\sum\limits_{t=1}^{n} \left(X_o^t - X_P^t \right)^2}{\sum\limits_{t=1}^{n} \left(X_o^t - \overline{X}_o \right)^2} \tag{25}$$

where n denotes the number of data, and X_o^t and X_p^t correspond to the observed and simulated runoff at time t, respectively. $\overline{X}_o$ denotes the mean of the observed values. A value equal to one corresponds to a perfect match of simulated runoff to the observed data. The range of E lies between 1.0 (perfect fit) and −1.0. An efficiency of 0 indicates that the model predictions are as accurate as the mean of the observed data, whereas an efficiency of lower than zero indicates that the simulated value is not as good as the observed value (Krause et al. 2005).

As it is shown in Table 7, the improvement of the MLP model in comparison with the IHACRES model is 30% and 60% based on MAE and RMSE respectively. As for the Nash–Sutcliffe efficiency coefficient, in calibration period, both of the models have the same performance, but in the validation period, the MLP predictions are more reliable than IHACRES model, since the efficiency of the IHACRES simulation is less than zero.

4.4 Determination of Probable Drought Periods

The results of the streamflow simulation showed that the average streamflow during 2005–2023 in comparison with historical data (1986–2004) will decrease about 13% but during 2024–2042 it will increase about 17% in the study area. In addition, the results show that in the future, the time of maximum streamflow occurrence at the OG station will be shifted from April to June, which should be considered in deriving reservoir operation policies.

Table 7 Comparison between IHACRES and modified IHACRES-ANN output

Period	Model	R^2 (%)	RMSE (MCM)	MAE (MCM)	E
Calibration	IHACRES	55	2.19	1.43	0.56
	MLP	73	1.644	1.06	0.49
Validation	IHACRES	60	5.60	3.83	−0.85
	MLP	63	2.30	1.50	0.15

The pre-assessment of reservoir operation during the drought periods plays an important role in mitigation of the expected damages. Therefore, projecting probable drought periods in future and their characteristics is necessary. In this study, drought indices of SPI, SWSI and RDI are calculated to determine the probable drought periods in future.

The SPI is formulated by Mckee et al. (1993). This index assigns a single numeric value to the precipitation which can be compared across regions with markedly different climates. Technically, the SPI is the number of standard deviations that the observed value would deviate from the long-term mean, for a normally distributed random variable. Since precipitation is not normally distributed, a transformation is first applied so that the transformed precipitation values follow a normal distribution.

The Surface Water Supply Index (SWSI) is a predictive indicator of total surface water availability within a watershed. SWSI values are scaled from +4.2 (abundant supply) to −4.2 (extremely dry) with a value of zero (0) indicating media water supply as compared to historical analysis. The formulation of SWSI is given as

$$SWSI = \frac{P - 50}{12} \tag{25}$$

where P is the single probability of summed expected streamflow and current reservoir storage (Garen 1993).

The RDI index is developed by Tsakiris and Vangelis (2005). In this index, the ratio of precipitation over potential evapotranspiration (ET_p) is used as a representative of the wetness condition for different time scales in the study region. For yearly time scale this index is estimated as follows:

$$\alpha_0^{(i)} = \frac{\sum_{j=1}^{12} P_{ij}}{\sum_{j=1}^{12} PET_{ij}}, i = 1, \dots N \quad and \quad j = 1, \dots 12 \tag{26}$$

$$RDI_{st(k)}^{(i)} = \frac{y_k^{(i)} - \overline{y}_k}{\widehat{\sigma}_{yk}} \tag{27}$$

where P_{ij} and PET_{ij} are precipitation and potential evapotranspiration of the jth month of the ith year and N is the total number of years of the available data. $\alpha_0^{(i)}$ corresponds to the initial value of the index. $RDI_{st(k)}^{(i)}$ is the Standardized form of RDI which is interpreted similarly to SPI for determining the wetness condition. y_k is the $\ln\alpha_0^{(i)}$, $\overline{y}_k$ is the arithmetic mean and $\widehat{\sigma}_{yk}$ is the standardized deviation (Tsakiris et al. 2006).

In addition to these drought indices, the variations of streamflow are considered to find the probable drought periods in the future. The identified drought periods with duration more than 2 years are considered as possible severe drought periods in future for examining the hedging rules performance on Sattarkhan reservoir operation. The characteristics of the identified drought periods are presented in Table 8. The severity of droughts is determined by the summation of water shortages or negative values of RDI in the drought period. RDI is a better representation of drought condition in the study region because it considers both rainfall and evapotranspiration. Among the four identified drought periods in Table 8, the 3rd and 4th drought events which are the most severe and longest drought periods, are

considered for developing hedging rules. If the hedging rule could mitigate these severe water shortages then it can better handle low flow conditions.

4.5 Application of Hedging Rules

The Sattarkhan reservoir has been operating since 2000, therefore the operating data between 2000 and 2004 has been used for calibrating the reservoir hedging rules considering a constant seasonal pattern of water demand.

In developing the optimization model of reservoir operation, two alternatives are considered as follows:

- Alternative 1: All of the water demands have been assumed to be in one group regarding the objective functions by the assumption that the environmental demand is fully supplied (the minimum reservoir release is set equal to instream (environmental demand)).
- Alternative 2: Two groups of water users have been considered in the objective function: a) the domestic, industrial and instream (environmental demand) (Public demand); b) the agricultural water demand. It is assumed that at least the instream (environmental demand) in the first group and the water demand of orchards in the second group must be supplied.

The results show that the performance of hedging in water allocation in both of the alternatives is almost the same. However, the reservoir storage volume in the second alternative is 30% more than the reservoir storage of the first alternative during the operation horizon. Indeed, the developed hedging rule in the second alternative is more effective in maintaining the water in the reservoir to be used in the forthcoming dry periods. Therefore for the rest of this study the second alternative is considered to achieve the optimal operating policies in the future years.

Different combinations of rationing factors are considered for water allocation to two groups of water users in developing hedging rules. The ranges of rationing factors lie between 0 and 1. In this study, the optimization model has been run for different combinations of public and agricultural demands. Within the ranges of demand rationing factors, more than 30 combinations are defined for model development. The six most appropriate combinations of these factors which have better performance in developing reservoir operation schemes are presented by number 1–6 in Table 9. In these combinations α_1, α_2 vary for public demand and agricultural demand in the range of 0.8–1 and 0.3–0.7, respectively. The monthly average of water supply and water shortage during the operation period for each of these combinations are also presented in this table. S_R, Sh_P and Sh_A variables in Table 9 refer to the reservoir storage volume and the percentages of water

Table 8 Characteristics of the possible severe drought periods in the future

Drought period No.	Duration (year)	Severity	RDI (Magnitude)	SPI (Severity)	SWSI (Severity)
1	2	44	2.6	3.4	9.27
2	5	90	3.5	3.89	9.23
3	8	105	18.8	3.14	9.42
4	15	425	33.5	5.58	18.14

shortage in public and the agricultural demands, respectively. As public demand has a priority over agricultural demand; therefore, models 3 and 5 which have the least shortage in the public demand supply have been selected as the better models.

The values of rationing factors play an important role in determination of the percentage of water shortage in different groups of consumers. Therefore, in models 3 and 5 which have the same rationing factors as in public demand, the increase of rationing factors of agricultural demand has decreased the amount of water shortage from 46.2% to 38.55%. In this case the amount of water shortage in public demand has been increased from 0.26% to 0.36%.

Although model 3 provides more water storage in comparison with model 5, due to less water shortage of model 5 in agricultural group, model 5 has been selected as the best model in this study.

The selected hedging model can identify the drought periods and trigger the reservoir operation accordingly. The operating model limits the water supply in normal years and stores water for the coming drought years. This way, the expected damages in the drought periods decrease considerably. It should be noted that in the developed model the release is always more than the environmental demand due to the constraint considered for minimum release from the reservoir.

4.6 Development of Policies for Dry Periods

For estimation of future water demand, the data provided in Karamouz (2010) are used. Regarding this study, the irrigation efficiency and water loss in the domestic section have been considered to be equal to 70% and 10%, respectively and the variations of demand in future for different sectors are given in Table 1.

Based on the estimated water demands for the future (Table 1), the water demand is almost constant during the months of November to March. After these months, the demand increases to reach its maximum value in July and then declines. The water demand gets its maximum value in July because of the high temperature resulting in the high amount of evaporation and transpiration; moreover, the most sensitive growth period of plants to water deficit is in this month.

The operation curves are developed for the 3rd and 4th drought events, which are the most severe and longest drought periods, based on Eqs. 5 to 15 and rationing factors of model 5 in Table 9. The results of the reliability of chosen dry periods in each year are given in Table 10. Also, the results of the application of hedging rules with parameters of

Table 9 The results of sensitivity analysis on the rationing factors of different water users

Model No.	Public demand		Agriculture demand		S_R (MCM)	Sh_P (%)	Sh_A (%)
	$\alpha1$	$\alpha2$	$\alpha1$	$\alpha2$			
1	0.9	0.8	0.7	0.4	42.59	8.69	33.58
2	0.95	0.85	0.65	0.35	42.36	5.09	32.80
3	1	0.9	0.6	0.3	41.91	0.26	46.20
4	0.9	0.8	0.6	0.3	45.51	9.32	42.31
5	1	0.9	0.7	0.4	39.78	0.36	38.55
6	0.95	0.85	0.7	0.4	41.35	4.52	38.00

model 5 to the Sattarkhan reservoir during the 3rd and 4th drought events as well as SOP releases are shown in Fig. 7. This figure shows that the allocated water of the hedging rule in the 3rd drought period is close to the water demand in most of the months. According to this figure, in the 4th drought period the simulated releases do not satisfy the water demand primarily during the summer and spring. In this period, the average, maximum, and minimum monthly water shortage are equal to 1.9 MCM 4.5 MCM (in May), and 0.1 MCM (in March), respectively. There is an almost constant water shortage in each month which shows the stability of system operation during the drought periods which is desirable in developing drought damage mitigation programs in the study area. Also the comparison between the hedging rule results with the standard operation rule during (2000–2004) shows that using the hedging rules for water supply is more compatible with the demand variation and as a result the intensity of water shortages has been decreased. This figure shows that hedging rule has a much better performance in water allocation during drought periods in comparison with SOP. Using SOP serious water shortages especially in periods of high water demand could be resulted.

The analysis of monthly results of application of hedging rules and SOP in 3rd and 4th dry periods (Fig. 8) shows that by application of hedging rules more reasonable and sustainable water supply scheme during drought periods can be achieved. Using hedging rules in two considered drought periods, has decreased the maximum percentage of water shortage in 3rd and 4th dry periods from 0.93 and 0.88 to 0.82 and 0.78, respectively.

Table 10 The reliability of water demand supply during 3rd and 4th dry periods

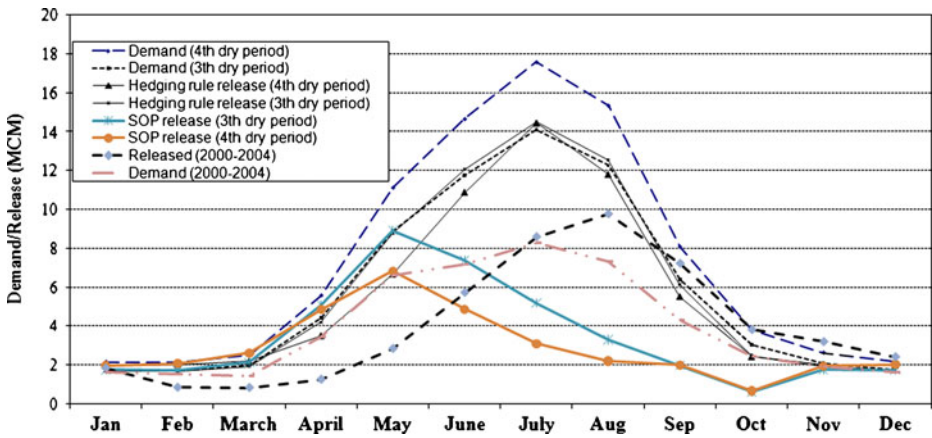| Drought Period No.	Year	Reliability (%)
3	1	46
	2	60
	3	61
	4	47
	5	51
	6	48
	7	45
	8	59
4	1	77
	2	46
	3	36
	4	35
	5	40
	6	33
	7	34
	8	38
	9	34
	10	33
	11	40
	12	33
	13	31
	14	29
	15	29

Fig. 7 The monthly reservoir release in comparison with water demands in 3th and 4th dry periods

5 Conclusion

Water resources planners and decision makers in recent years are paying more attention to preparedness of systems to deal with water shortages before drought occurrence. In this approach, the probable drought risks from magnitude, severity and duration aspects are projected before occurrence of disaster and the system is prepared to deal with them through development of appropriate policies. The water resources system readiness in dealing with water shortage could highly decrease the water deficit and socio-economical problems. This has become more important in recent years because of the climate change impacts resulting in increased frequency and severity of droughts.

In this paper, an integrated drought management approach in dealing with drought events with various characteristics under climate change impacts is developed. The proposed algorithm has been applied to the Aharchay basin in the northwestern part of Iran. The results of climate change studies show a decreasing trend of rainfall and runoff in the study area that will affect agricultural based economical activities as well as people's lifestyle in the region. This also results in increasing water shortage periods and therefore necessity of drought mitigation strategies. In the two 20 year periods considered, in the second period, there is a severe water shortage in spring and summer that water demand cannot be supplied. To manage real time operation of Sattarkhan reservoir, hedging rules have been applied to reduce water shortages. This results in a more stable water supply
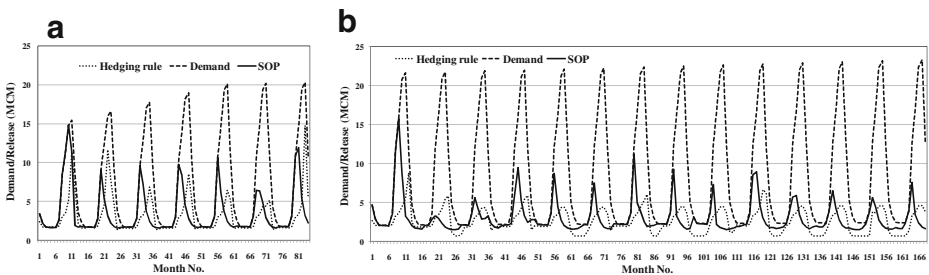

Fig. 8 The monthly time series of reservoir release under application of SOP and Hedging rule (**a**) at the 3rd drought period (**b**) at the 4th dry period

scheme for drought periods and provides a lead time to apply water conservation strategies for the better use of the available water resources.

The results of this study show the successful application of the proposed algorithm in mitigating the severe drought periods in the region considering climate change impacts. The proposed algorithm can be applied to other basins with different characteristics but special care should be taken to incorporate the regional characteristics and the specific priorities in water supply and allocation in adopting the proposed algorithm. Applying this algorithm could decrease the scarcity of water supply in a region and serve as a useful tool in sustainable management of water resources.

References

Abbaspour M, Sabetraftar A (2005) Review of cycles and indices of drought and their effect on water resources, ecological, biological, agricultural, social, and economical issues in Iran. Int J Environ Stud 62(6):709–724

Bayazit M, Unal NE (1990) Effects of hedging on reservoir performance. Water Resour Res 26(4):713–719

Bower BT, Hufschmidt MM, Reedy WW (1962) Operation procedures: their role in the design of water-resources systems by simulation analysis. In: Maass A, Hufschmidt MM, Dorfman R, Thomas HA Jr, Marglin SA, Fair GM (eds) Design of water resources systems. Harvard University Press, Cambridge

Brown MB, Forsythe AB (1974) Robust tests for the equality of variances. J Am Stat Assoc 69(346):364–367

Carter TR, Parry ML, Harasawa H, Nishioka S (1994) IPCC Technical Guidelines for Assessing Climate Change Impacts and Adaptations for Policy Makers and a technical Summary. Department of Geography, University College London, UK, and the Center for Global Environmental Research, National Institute for Environmental Studies, Japan, 59 pp

Clausen B, Pearson CP (1995) Regional frequency analysis of annual maximum streamflow drought. J Hydrol 173(1–4):111–130

Conover WJ (1980) Practical nonparametric statistics, 2nd edn. Wiley, New York, 490 pp

Dibike YB, Coulibaly P (2005) Hydrologic impact of climate change in the Saguenay watershed: comparison of downscaling methods and hydrologic models. J Hydrol 307(1–4):145–163

Draper AJ, Lund JR (2004) Optimal hedging and carry-over storage value. J Water Resour Plan Manag 130 (1):83–87

Garen DC (1993) Revised surface water supply index for Western United States. J Water Resour Plan Manag 119(4):437–454

Harpham C, Wilby RL (2005) Multi-site downscaling of heavy daily precipitation occurrence and amounts. J Hydrol 312:235–255

Hashimoto T, Stedinger JR, Loucks DP (1982) Reliability, resiliency and vulnerability criteria for water resource system performance evaluation. Water Resour Res 18(1):14–20

Hassan H, Aramaki T, Hanaki K, Matsuo T, Wilby RL (1998) Lake stratification and temperature profiles simulated using downscaled GCM output. Water Sci Technol 38(11):217–226

Hay LE, Wilby RL, Leavesley GH (2000) A comparison of delta change and downscaled GCM scenarios for three mountainous basins in the United States. J Am Water Resour Assoc 36(2):387–398

Hingray B, Mezghani A, Buishand TA (2007) Development of probability distributions for regional climate change from uncertain global mean warming and an uncertain scaling relationship. Hydrol Earth Syst Sci 11(3):1097–1114

IPCC (2001) Technical Summary in Climate Change 2001: impacts, adoptions, mitigation of climate change: scientific-technical analysis. In: Watson RT, Zinyowera MC, Moss RH (eds) Contribution of working group II to the second assessment of the intergovernmental panel on climate change. Cambridge University Press, UK, 878 pp

Jakeman AJ, Hornberger GM (1993) How much complexity is warranted in a rainfall–runoff model? Water Resour Res 29(8):2637–2649

Karamouz M (2010) Revisiting water supply and demand, and drought management in the Aharchay Watershed, the East Azarbyjan water authority, Iran (In Farsi)

Karamouz M, Araghinejad Sh (2008) Drought mitigation through long-term operation of reservoirs: case study. J Irrig Drain Eng 134(4):471–478

Karamouz M, Torabi S, Araghinejad Sh (2007) Case study of monthly regional rainfall evaluation by spatiotemporal geostatistical method. J Hydrol Eng 12(1):97–108

Karamouz M, Rasouli K, Nazif S (2009) Development of a hybrid index for drought prediction: case study. J Hydrol Eng 14(6):617–627

Khalili D, Farnoud T, Jamshidi H, Kamgar-Haghighi AA, Zand-Parsa Sh (2011) Comparability analyses of the SPI and RDI meteorological drought indices in different climate zones. Water Resour Manag 25 (6):1737–1757

Krause P, Boyle DP, Base F (2005) Comparison of different efficiency criteria for hydrological model assessment. Adv Geosci 5:89–97

Lund JR, Guzman J (1996) Developing seasonal and long-term reservoir system operation plans using HEC-PRM. Technical Report RD-40, Hydrologic Engineering Cente. U.S. Army Corps of Engineer, Davis, Calif

Massah Bavani AR (2006) Risk assessment of climate change and its impact on water resources, Case-Study: Zayandeh Rud Basin Isfahan. Ph.D. Dissertation, Department of Civil Engineering. Tarbiat Modaress University, 192 pp (In Farsi)

Mays LW (2003) Urban water supply management tools. McGraw Hill, New York, 208 pp

McKee TB, Doesken NJ, Kleist J (1993) The relationship of drought frequency and duration of time scales. Eighth Conference on Applied Climatology. American Meteorological Society, Anaheim CA, pp 179–186

Morid S, Smakhtin V, Moghaddasi M (2006) Comparison of seven meteorological indices for drought monitoring in Iran. Int J Climatol 26:971–985

Prudhomme C (2006) GCM and downscaling uncertainty in modeling of current river flow: why is it important for future impacts? Proceedings of the 5th FRIEND World Conference. Havana, IAHS Publication, 308, 375–381

Sajjad Khan M, Coulibaly P, Dibike Y (2006) Uncertainty analysis of statistical downscaling methods. J Hydrol 319(1–4):357–382

Shih JS, ReVelle C (1994) Water-supply operations during drought: continues hedging rule. J Water Resour Plan Manag 120(5):613–629

Spearman JR, Baugh J, McCoy MJ (2004) Use of sub-grid approaches in the modeling of estuaries with Salt Marsh Systems. HR Wallingford Report TR138, 64 pp

Srinivasan K, Philipose MC (1996) Evaluation and selection of hedging policies using stochastic reservoir simulation. Water Resour Manag 10(3):163–188

Tabrizi AA, Khalili D, Kamgar-Haghighi AA, Zand-Parsa Sh (2010) Utilization of time-base meteorological droughts to investigate occurrence of streamflow droughts. Water Resour Manag 24(15):4287–4306

Tsakiris G, Vangelis H (2005) Establishing a drought index incorporating evatranspiration. European Water 9 (10):3–11

Tsakiris G, Pangalou D, Vangelis H (2006) Regional drought assessment based on the Reconnaissance Drought Index (RDI). Water Resour Manag 21(5):821–833

Tu MY, Hsu NS, Yeh WG (2003) Optimization of reservoir management and operation with hedging rules. J Water Resour Plan Manag 129(2):86–97

Vangelis H, Spiliotis M, Tsakiris G (2010) Drought severity assessment based on bivariate probability analysis. Water Resour Manag 25(1):357–371

Vidal JP, Wade SD (2008) Multimodel projections of catchment-scale precipitation regime. J Hydrol 353(1–2):143–158

Wigley TML, Jones PD (1985) Influence of precipitation changes and direct CO_2 effects on streamflow. Nature 314:149–151

Wigley TML, Jones PD, Briffa KR, Smith G (1990) Obtaining subgrid scale information from coarse-resolution general circulation model output. J Geophys Res 92:1943–1953

Wilby RL, Harris I (2006) A framework for assessing uncertainties in climate change impacts: low-flow scenarios for the River Thames. Water Resour Res 42:W02419. doi:10.1029/2005WR004065

Wilby RL, Hay LE, Leavesle GH (1999) A comparison of downscaled and raw GCM output: implications for climate change scenarios in the San Juan River Basin, Colorado. J Hydrol 225(1–2):67–91

Wilby RL, Hay LE, Gutowski WJ, Arritt RW, Takle ES, Pan Z, Leavesley GH, Clark MP (2000) Hydrological response to dynamically and statistically downscaled climate model output. Geophys Res Lett 27:1199–1202

Wilby RL, Dawson CW, Barrow EM (2002) SDSM—a decision support tool for the assessment of regional climate change impacts. Environ Model Softw 17:147–159